[American Journal of Science, Vol. 267, May, 1969, P. 609-626]

# MELTING REACTIONS IN THE SYSTEM $KAlSi_3O_8$-$SiO_2$-$H_2O$ TO 18.5 KILOBARS

I. B. LAMBERT,* J. K. ROBERTSON, and P. J. WYLLIE

Department of the Geophysical Sciences,
The University of Chicago, Chicago, Illinois 60637

ABSTRACT. Synthetic sanidine with composition $Or_{95}Ab_5$ was crystallized from gel, and a portion was mixed with 15 wt percent natural quartz. The sanidine and sanidine-quartz mixture were reacted with 30 to 40 wt percent water in sealed platinum capsules, using piston-cylinder apparatus. The melting relationships for these two crystalline mixtures, in the presence of excess water, were determined to 18.5 kb pressure. The divariant melting intervals located for each sample, along with the results of previous studies in the system $KAlSi_3O_8$–$SiO_2$–$H_2O$, provided good estimates of the positions of univariant curves for the two reactions: (a) Or + V $\rightleftharpoons$ L, and (b) Or + Qz + V $\rightleftharpoons$ L. Values for reaction (a) are 5 kb–875°C; 10 kb–825°C; 15 kb–795°C; 20–775°C. Values for reaction (b) are 5 kb–740°C; 10 kb–710°C; 15 kb–700°C; 20 kb–697°C. Muscovite was present in trace amounts in all runs, including those quenched from conditions well above its maximum temperature stability limit, but it was not found enclosed in glass. We therefore conclude that muscovite was a deposit from the vapor phase. Schematic phase diagrams for the system $K_2O$–$Al_2O_3$–$SiO_2$–$H_2O$ indicate that muscovite would not be expected as a stable liquidus phase for mixtures on the join $KAlSi_3O_8$–$SiO_2$–$H_2O$ at pressures less than 10 kb.

## INTRODUCTION

There have been many experimental studies of the melting relationships of minerals and rocks in the presence of excess water at pressures up to 10 kb, but most studies at higher pressures have been conducted with dry samples or in the presence of a small but unknown proportion of water. In an effort to test recent proposals that some igneous rocks of the calc-alkaline series may be primary magmas from the mantle (see Green and Ringwood, 1968, for review), we have extended phase equilibrium studies for plutonic rock series into the pressure range corresponding to upper mantle conditions, in the presence of excess water. The conditions of magma generation in the mantle, in general, must involve only traces of water, but the phase relationships determined in the presence of excess water provide limiting conditions for comparison with the results in the dry systems. The curve for the beginning of melting of a granite in the presence of excess water to 30 kb (Boettcher and Wyllie, 1968a) provides a lower temperature limit for the existence of magmas in the upper mantle.

In order to provide a basis for interpretation of the complex phase relationships in the natural rock systems, it is also necessary to extend the phase relationships in simple silicate-water systems to upper mantle pressures, above 10 kb. Boettcher and Wyllie (1967; 1969a) have determined the water-saturated phase relationships in the system $NaAlSiO_4$–$SiO_2$–$H_2O$ to 35 kb pressure. This paper is concerned with the system $KAlSi_3O_8$–$SiO_2$–$H_2O$ to 18.5 kb pressure. Together these results provide boundaries for the simplified granite system, $NaAlSi_3O_8$(Ab)–$KAlSi_3O_8$(Or)–$SiO_2$(Qz)–$H_2O$, at upper mantle pressures.

---

* Present address: Baas Becking Laboratory, Bureau Mineral Reseources Building, Anzac Parade, Canberra, AUSTRALIA

Goranson (1938) was the first to obtain quantitative results on melting relationships in silicate-water systems, and he studied the system Or–$H_2O$ to 4 kb. Yoder, Stewart, and Smith (1957) published the solidus temperature at 5 kb in the system Or–$H_2O$. Tuttle and Bowen (1958) studied Qz–$H_2O$ and parts of the system Or–Qz–$H_2O$ to 2 kb. The univariant melting curve in the system Or–Qz–$H_2O$ was measured to 4 kb by Shaw (1963) and to 10 kb by Luth, Jahns, and Tuttle (1964). Spengler (ms) studied Or–$H_2O$ to 6.5 kb. Scarfe, Luth, and Tuttle (1965) determined the phase relationships in the system $KAlSiO_4$(Ks)-$SiO_2$–$H_2O$ to 10 kb, with special reference to the relationships between Or, Leucite (Lc), and liquid. Seki and Kennedy (1965) reported that in the range 10 to 34 kb orthoclase reacts with water to form muscovite plus one or more fluid phases, which indicates that the system Or–Qz–$H_2O$ does not remain ternary above 10 kb; the studies of Segnit and Kennedy (1961) with muscovite-quartz mixtures may therefore be relevant. Some results are available for the dry system at pressures above 10 kb. Lindsley (1966) described the melting relations of $KAlSi_3O_8$ up to 40 kb, and he extended the composition range to Or–Ks in 1967. Luth (1968) presented phase relationships for the system Or–Qz to 20 kbars.

## EXPERIMENTAL METHOD

*Starting materials.*—Our starting materials were natural quartz and sanidine crystallized hydrothermally from a finely ground gel. The gel was supplied by D. H. Watkinson, who had prepared a series of gels in the system Ab–Or, using standard procedures (Luth and Ingamells, 1965). A dehydrated portion of the sodium-stabilized "Ludox" used as a source of $SiO_2$ for the gels was analyzed by C. O. Ingamells, and it contained 1.3 wt percent $Na_2O$. This was taken into account in making up the gels, and the potassium end-member of the series therefore contained 0.86 wt percent $Na_2O$, which is equivalent to 5 wt percent Ab in solution. Electron microprobe analysis of the crystallized orthoclase gel confirmed that the crystals did have the composition $Or_{95}Ab_5$. A Nonius Guinier camera was used to take an X-ray powder photograph of the sanidine starting material, with $KBrO_3$ internal standard (Orville, 1963), and the composition determined from the position of the $\bar{2}01$ line was likewise $Or_{95}Ab_5$.

*Apparatus and procedure.*—The starting materials were weighed into platinum tubes sealed at one end, and the other end was then welded in a carbon arc. All runs were made in a solid-medium, piston-cylinder device based on the design of Boyd and England (1960), using a half-inch diameter bomb with hardened steel liner. This apparatus was calibrated for pressure and temperature as described by Boettcher and Wyllie (1968b). Temperatures, measured with chromel-alumel thermocouples, were precise to ± 5°C and are considered accurate to ± 10°C. No correction was applied for the effect of pressure on the emf of the thermocouple. All pressures have been corrected for friction, which has been taken as —8 percent in the temperature range studied, and they are considered accurate to ± 5 percent in the runs at 9 kb and above. Wyllie and Boettcher (1969) studied a univariant reaction in the system $CaO$–$CO_2$–$H_2O$ ($dP/dT \approx 170$ bars/°C) and found that at pressures as low as 3.6 kb the corrected piston-cylinder runs agreed with the univariant curve defined by runs in cold seal pressure vessels. Sample capsules were weighed before and after each run, whenever the condition of the capsule after a run was suitable, and capsules that had lost water were discarded.

*Identification of phases.*—The compositions of phases recognized in runs on the two experimental joins are shown by the schematic phase diagrams of figure 1. There are isobaric diagrams for the system Ks–Qz–$H_2O$ after figures 4A and 4C of Scarfe, Luth, and Tuttle (1965) modified to include the results of Kennedy and others (1962) on the compositions of liquid and vapor phases in the system $SiO_2$–$H_2O$. Note that at 6 kb, the compositions of liquid and vapor in Qz–$H_2O$ are closer together than in the bounding system Ks–$H_2O$ (fig. 1B).

The phases present at run conditions included crystals of sanidine (Or) and quartz (Qz), liquid (silicate liquid saturated with $H_2O$), and vapor (a dense, aqueous fluid phase containing dissolved solid components). The phase assemblage at run conditions was determined by standard optical and X-ray study of the quenched materials. Original crystalline phases were preserved during the quench; liquids (L) quenched to glasses; and the vapor phase (V) quenched to water and precipitated solid materials. The microscopic character of the glass and vapor phase deposits was similar to that described by Boettcher and Wyllie (1968a) for the system granite-water. Muscovite occurred in trace amounts in all quenched runs, even in those quenched from conditions well above the known stability limits of muscovite or of the muscovite-

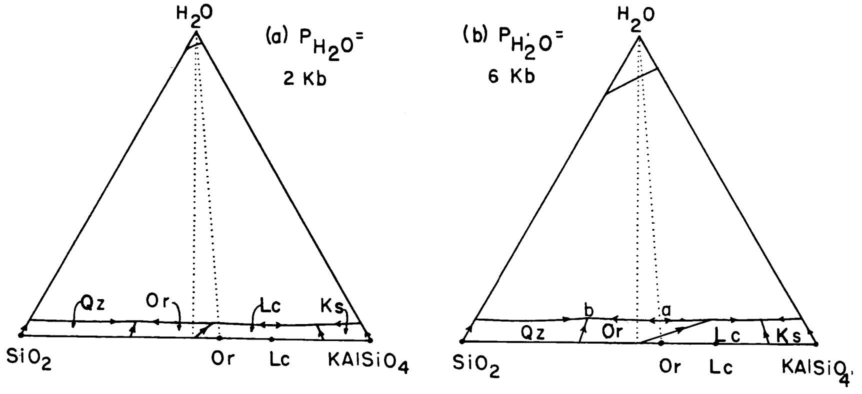

Fig. 1. Schematic isobaric equilibrium diagrams for the system Ks–Qz–$H_2O$ at 2 kb and 6 kb, modified after figures 4A and 4C of Scarfe, Luth, and Tuttle (1965) to include the results of Kennedy and others (1962) on the compositions of liquids and vapors in the system Qz–$H_2O$. Liquid compositions a and b can be located in figure 5 for the system $K_2O$–$Al_2O_3$–$SiO_2$–$H_2O$; they are the liquids involved in reactions (a) and (b) plotted in figures 4 and 6.

quartz assemblages. Furthermore, muscovite was never found enclosed in glass, as were the primary crystals of sanidine and quartz. Therefore, we conclude that the muscovite is a quench product.

Kennedy and others (1962) reported a second critical end-point in the system $SiO_2$–$H_2O$ at a pressure of 9.7 kb at 1080°C, with liquid and vapor phases becoming identical in composition and physical properties; the composition of the critical fluid was approximately 25 wt percent $SiO_2$ (but see Stewart, 1967). Thus, if figure 1B were modified for a pressure of 9.7 kb, the liquid field boundary and the vapor field boundary would be connected together smoothly through the critical point on the join $SiO_2$–$H_2O$. At higher pressures, this binary critical fluid becomes ternary as $KAlSiO_4$ is dissolved in it, and the miscibility gap between liquid and vapor phases extending from the system Ks–$H_2O$ would then close via a critical point within the ternary system, rather than terminating at another miscibility gap in the system $SiO_2$–$H_2O$. Phase relationships of this type have been described by Boettcher and Wyllie (1969b). This is relevant to the present study, because with increasing pressure above 9.7 kb, the ternary critical point moves toward the join Or–$H_2O$, and the compositions of liquids and vapors occurring on this join probably approach each other. The effect was noticed for mixtures on the join passing through the triangle Or–Qz–$H_2O$ (see fig. 1). In runs at 13.8 kb pressure, distinction between glass and quenched vapor phase deposits was made with certainty, whereas in runs at 18.5 kb, identification of the first trace of glass and its distinction from vapor phase deposits became more difficult.

Stewart (1967) obtained results in the system $SiO_2$–$H_2O$ indicating that the second critical end-point lies at some pressure higher than 10 kb and probably at a temperature lower than 1055°C; at 10 kb, he found that the liquid contained 22 wt percent $H_2O$ and the vapor phase 38 wt percent $SiO_2$. However, whatever the position of the critical end-point in the system $SiO_2$–$H_2O$ may be, his results indicate that liquid and vapor phase compositions in the system Or–Qz–$H_2O$ should approach each other quite closely by 18.5 kb pressure.

## EXPERIMENTAL RESULTS

*General remarks.*—Phase relationships in the join Ks–Qz–$H_2O$ are presented as ternary in figure 1 and in similar diagrams to 10 kb by Scarfe, Luth, and Tuttle (1965). It is thus assumed that the compositions of liquid and vapor phases remain within this triangle. The assumption is justified within the limits of experimental detection at the lower pressures, but with increasing pressure, increasing departure from strict ternary relationships may be anticipated. The appearance of muscovite as a quench product in our experiments, and possibly as a primary phase in other experiments on the join Or–$H_2O$ (Seki and Kennedy, 1965), is a reminder of the fact that the join is a section through the quaternary system $K_2O$–$Al_2O_3$–$SiO_2$–$H_2O$ (see fig. 5).

Dry orthoclase melts incongruently to leucite plus liquid, as shown in figure 1. In the join Or–$H_2O$ at pressures below 2.6 kb (Goranson, 1938), orthoclase also yields leucite when melting begins, as shown in figure 1A. However, figure 1B shows that at higher pressures, orthoclase melts congruently in the presence of excess water. Therefore, within the experimental range of this study, the join Or–$H_2O$ is treated as a binary system when excess water is present. This is valid only if the compositions of the liquid and vapor phase produced from mixtures on the join Or–$H_2O$ remain on this join; if the vapor phase composition departs from the join but remains within the triangle Ks–Qz–$H_2O$, then the join Or–$H_2O$ must be considered as a join through the ternary system, and instead of a univariant melting curve the join Or–$H_2O$ will intersect a divariant melting interval. Phase relationships of this type were described and illustrated by Boettcher and Wyllie (1969b). If the composition of the vapor phase leaves the triangle with increasing pressure, as it must if muscovite becomes a primary phase (Seki and Kennedy, 1965), then the join Or–$H_2O$ must be considered simply as a composition join through a quaternary system.

Considerations of this type are insignificant for experiments in silicate-water systems at lower pressures, where the composition of the vapor phase can be treated as if it were $H_2O$ because of the low solubility of solids. Narrow divariant melting intervals may appear to be univariant curves within the limits of experimental measurement. However, at 10 kb pressure, the solubility of solids in the vapor phase in silicate-water systems is in the range of 8 to 10 wt percent, and nonstoichiometric solution is to be expected in many systems (Burnham, 1967).

Our experiments were aimed at locating two of the melting reactions illustrated in figure 1:

$$\mathrm{Or} + \mathrm{V} \rightleftharpoons \mathrm{L(a)}, \text{ and } \mathrm{Or} + \mathrm{Qz} + \mathrm{V} \rightleftharpoons \mathrm{L(b)}$$

These have been treated in previous publications as binary and ternary, respectively, at pressures up to 10 kb, with the implication that the vapor phases remain on the joins Or–$H_2O$. However, most previous experimental investigations have suffered from the same problem as ours, namely, the presence of $Na_2O$ in small quantities in the source materials, with the result that the orthoclase starting material contained albite in solid solution. Therefore, what was measured experimentally were divariant melting intervals in the systems Or–Ab–$H_2O$ and Or–Ab–Qz–$H_2O$. Addition of a small proportion of Ab to the systems Or–$H_2O$ and Or–Qz–$H_2O$ may have a marked effect on the temperature of beginning of melting, but the univariant reaction curves are actually situated at only slightly higher temperatures than the measured melting intervals. This is illustrated by the results of Yoder, Stewart, and Smith (1957) for the system Or–Ab–$H_2O$ at 5 kb (their fig. 38). The aim of our experiments, therefore, was to determine the upper boundaries of divariant melting intervals, as well as the curves for the beginning of melting.

TABLE 1

Results of quenching experiments with crystalline sanidine ($Or_{95}$ $Ab_5$) in the presence of excess water

| Run No. | Wt percent water | Pressure Kbar | Temperature °C | Time Hours | Results* |
|---|---|---|---|---|---|
| 86 | 36 | 5 | 825 | 16 | Or + V |
| 71 | 31 | 5 | 836 | 18 | Or + L(tr) + V |
| 94 | 35 | 5 | 842 | 4.5 | Or + L + V |
| 95 | 35 | 5 | 845 | 3 | Or + L + V |
| 69 | 33 | 5 | 850 | 5.5 | Or + L + V |
| 59 | 39 | 5 | 860 | 20.5 | Or + L + V |
| 61 | 33 | 5 | 875 | 23.5 | L + V |
| 64 | 33 | 7.5 | 795 | 16 | Or + V |
| 62 | 33 | 7.5 | 810 | 20.5 | Or + L + V |
| 35 | 35 | 9.3 | 783 | 3 | Or + V |
| 36 | 33 | 9.3 | 796 | 4 | Or + L(tr) + V |
| 33 | 36 | 9.3 | 800 | 3.5 | Or + L + V |
| 96 | 35 | 9.3 | 800 | 16.5 | Or + L + V |
| 32 | 33 | 9.3 | 820 | 17 | Or + L + V |
| 201 | 33 | 9.3 | 830 | 4 | L + V |
| 31 | 34 | 9.3 | 870 | 2 | L + V |
| 50 | 32 | 9.3 | 870 | 6 | [L + V] |
| Second stage | | 9.3 | 817 | 16 | Or(∼60 %) + L + V |
| 55 | 33 | 9.3 | 870 | 6 | [L + V] |
| Second stage | | 9.3 | 785 | 16.5 | Or + L(∼5 %) + V |
| 56 | 35 | 9.3 | 870 | 6.5 | [L + V] |
| Second stage | | 9.3 | 765 | 16.5 | Or + V |
| 38 | 34 | 13.8 | 760 | 5 | Or + V |
| 51 | 35 | 13.8 | 770 | 25 | Or + L(tr) + V |
| 63 | 33 | 13.8 | 785 | 5 | Or + L + V |
| 202 | 33 | 13.8 | 800 | 4 | L + V |
| 37 | 35 | 18.5 | 715 | 15 | Or + V |
| 34 | 38 | 18.5 | 745 | 17 | Or + V |
| 28 | 31 | 18.5 | 750 | 3 | Or + L(tr) + V |
| 31 | 34 | 18.5 | 760 | 3.5 | Or + L + V |
| 30 | 30 | 18.5 | 770 | 4.5 | Or + L + V |
| 29 | 32 | 18.5 | 780 | 2.5 | L + V |

Abbreviations: Or = sanidine; L = liquid (glass); V = vapor phase; (tr) = trace amount; [ ] = run not quenched.

* All runs contain a trace of muscovite.

*$KAlSi_3O_8$–$H_2O$*.—Our runs are listed in table 1 and plotted in figure 2. Between the two curves there is a divariant melting interval of 25° to 30°C, where the amount of liquid increases as the amount of sanidine decreases. Both curves were readily located using the crystalline starting material. The refractive indices of glasses are in the range 1.491 to 1.493 for all pressures studied. In order to check that crystals had not persisted above their stability limit because of incomplete reaction, we made reversal runs at 9.3 kb. Charges were taken to 870°, where previous runs confirmed that the phase assemblage was L + V, and then cooled to temperatures near the solidus (runs 50, 55, and 56 in table 1). At 25° above the solidus (as determined from crystalline charges) sanidine was precipitated confirming the position of the upper curve. At 10° below the solidus a small amount of glass persisted. At 25° below the solidus

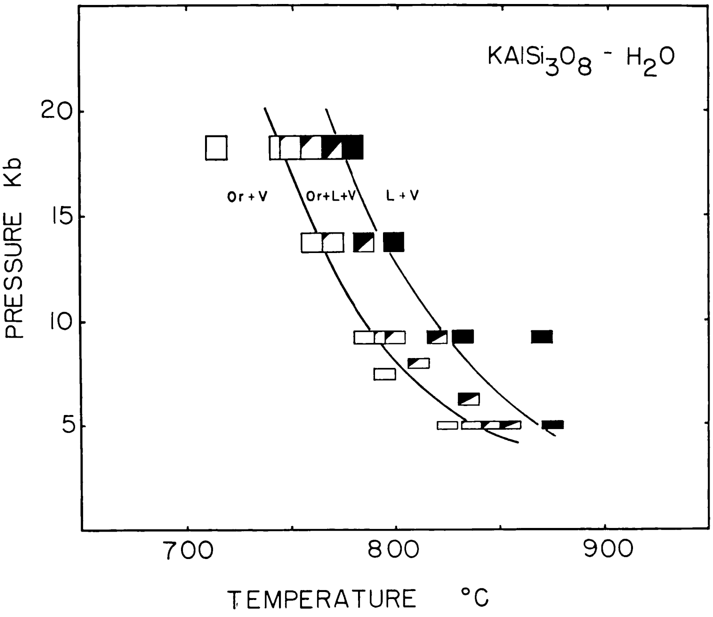

Fig. 2. Experimental results obtained for sanidine with composition $Or_{95}Ab_5$ in the presence of excess $H_2O$. The size of the run symbols represents the precision of temperature and pressure measurement. Note the divariant melting interval, Or + L + V.

all traces of glass disappeared, with sanidine and vapor as the only products. A noteworthy feature of the reversal runs was the large size of the crystals (up to 0.7 mm) which grew from the water-saturated liquid or glass when the temperature was lowered. In a few exploratory runs we managed to grow these large sanidine crystals at temperatures as low as 400°C.

*$KAlSi_3O_8$–$SiO_2$–$H_2O$.*—Our runs in this system are listed in table 2 and plotted in figure 3. There is a divariant melting interval for the assemblage Or + Qz + L + V, where the proportion of quartz decreases and the proportion of liquid increases with increasing temperature; the band is about 25° wide. The refractive indices of glasses in the runs from 7 to 13.8 kb are in the range 1.491 to 1.493. Up to 13.8 kb the curve for beginning of melting was sharply defined, but the difficulty of identification of the first trace of glass at 18.5 kb, and its distinction from vapor phase deposits, has already been mentioned. The upper boundary of the divariant interval for the mixture used was marked by the disappearance of quartz. Run 128 (table 2) was held first at a temperature in the stability field of Or + L + V and then cooled to 690°C within the divariant interval. A trace of quartz was recognized, but this was not a very convincing reversal of the upper boundary. Piwinskii (1968) found that runs of long duration were required to grow quartz from granitic liquids at lower pressures.

TABLE 2

Results of quenching experiments with a mixture of crystalline sanidine ($Or_{95}$ $Ab_5$, 85 wt percent) and quartz (15 wt percent) in the presence of excess water

| Run No. | Wt percent water | Pressure Kbar | Temperature °C | Time Hours | Results* |
|---|---|---|---|---|---|
| 67 | 33 | 7 | 685 | 18 | Or + Qz + V |
| 112 | 34 | 7 | 705 | 6 | Or + Qz(tr) + L + V |
| 70 | 33 | 7 | 705 | 25 | Or + Qz(tr) + L + V |
| 203 | 33 | 7 | 720 | 16 | Or + L + V |
| 46 | 40 | 9.3 | 670 | 6 | Or + Qz + V |
| 43 | 31 | 9.3 | 680 | 7 | Or + Qz + L(tr) + V |
| 41 | 33 | 9.3 | 690 | 4 | Or + Qz + L +V |
| 39 | 33 | 9.3 | 700 | 19 | Or + Qz(tr) + L + V |
| 113 | 33 | 9.3 | 700 | 19.5 | Or + Qz(tr) + L + V |
| 122 | 32 | 9.3 | 715 | 16.5 | Or + L + V |
| 128 | 33 | 9.3 | 730 | 2.5 | [Or + L + V] |
| Second stage | | 9.3 | 690 | 17 | Or + Qz(?tr) + L + V |
| 47 | 37 | 13.8 | 665 | 18 | Or + Qz + V |
| 48 | 38 | 13.8 | 680 | 18 | Or + Qz + L + V |
| 49 | 36 | 13.8 | 680 | 20 | Or + Qz + L + V |
| 52 | 35 | 13.8 | 695 | 22 | Or + Qz(tr) + L + V |
| 204 | 32 | 13.8 | 710 | 4 | Or + L + V |
| 42 | 32 | 18.5 | 650 | 15.5 | Or + Qz + V |
| 45 | 32 | 18.5 | 665 | 5 | Or + Qz + L(?tr) + V |
| 44 | 36 | 18.5 | 670 | 14 | Or + Qz + L + V |
| 53 | 38 | 18.5 | 680 | 22 | Or + Qz + L + V |
| 54 | 36 | 18.5 | 700 | 22 | Or + L + V |

Abbreviations: Or = sanidine; L = liquid (glass); V = vapor phase; (tr) = trace amount; [ ] = run not quenched; Qz = quartz; ? = uncertain.

* All runs contain a trace of muscovite.

*Comparison with previous studies and interpretation of results.*— Our results from figures 2 and 3 have been transferred to figure 4, with the divariant melting intervals shown as shaded bands.

The results of Shaw (1963) for the system Or–Qz–$H_2O$ are presented similarly as a band about 15° wide, extending between 0.5 and 4 kb. His runs define brackets for the interval at 2 and 4 kb but only the lower curve was bracketed at 0.5 and 1 kb. Shaw reported the curve for the beginning of melting as the univariant reaction. Two analyses of dehydrated portions of the Ludox that he used for preparation of Or gave values of 0.09 and 0.14 wt percent $Na_2O$. Chemical analysis of the Or gel indicated a content of 0.17 wt percent $Na_2O$, corresponding to about 1 percent Ab in solid solution. Therefore, it appears justifiable to conclude that the curve reported by Shaw as the univariant curve is in fact the beginning of a divariant interval, and the existence of the interval is not due simply to incomplete reaction of crystals. The univariant reaction then lies at a temperature slightly above the shaded interval.

Luth, Jahns, and Tuttle (1964) reported runs for the system Or–Qz–$H_2O$ within the pressure interval 6 to 10 kb, and the positions of their runs are shown in figure 4. Their Ludox contained 0.05 wt percent

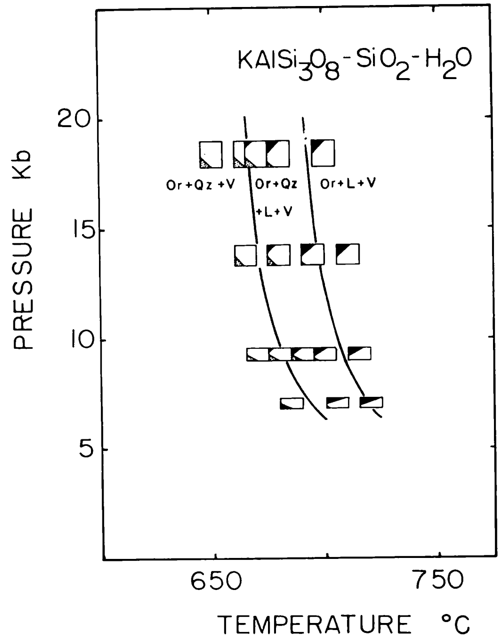

Fig. 3. Experimental results obtained for a mixture of sanidine ($Or_{95}Ab_5$) with 15 wt percent quartz, in the presence of excess water. The size of the run symbols represents the precision of temperature and pressure measurement. Note the divariant melting interval, Or + Qz + L + V. Key for run symbols: stipple—quartz, open—orthoclase, solid—liquid.

$Na_2O$, and they claim that this was present in the gel as excess $Na_2O$ (rather than being accommodated in the gel as $NaAlSi_3O_8$). "The minimum temperature at which a large amount of liquid was developed under a given pressure" was accurately located, and this provided the lower curve in figure 4 as their determination of the univariant reaction. However, their tabulated results indicate the existence of a four-phase interval, which is shaded in figure 4. Because of the short duration of their runs (0.5 or 1 hour), the shaded interval in this example may result from incomplete reaction.

In his study of the join Or–$H_2O$, Spengler (ms) used dehydrated gel containing 0.87 wt percent $Na_2O$. This is the same as for the gel used in our experiments, and it corresponds to about 5 wt percent Ab. His tabulated runs between 3 and 6 kb pressure indicate the existence of the shaded three-phase interval Or + L + V shown in figure 4. However, the use of gel as a starting material produced complications (see Shaw, 1963, for discussion), and Spengler concluded that the uncertainty of the "actual saturation-liquidus temperature is ± 15°C irrespective of the uncertainty of knowing the temperature of each run to better than ± 5°C".

Yoder, Stewart, and Smith (1957) presented a single point at 876°C and 5 kb for the univariant curve in the system Or–$H_2O$, using glass as

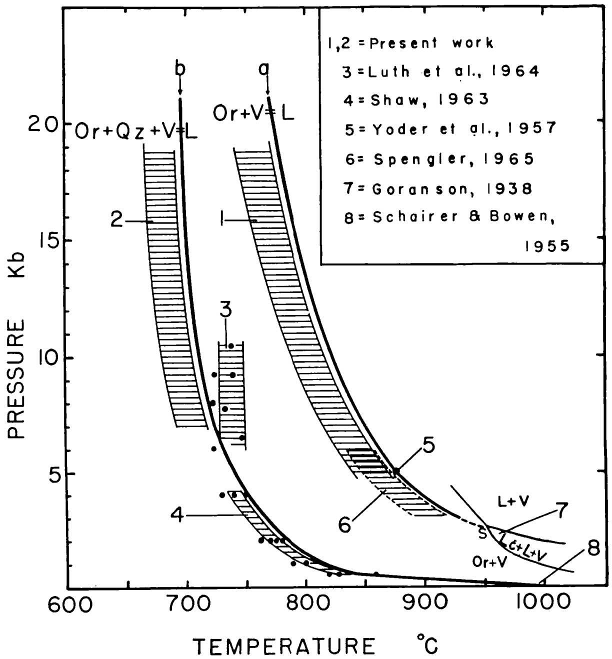

Fig. 4. Experimental results from figures 2 and 3 compared with previous results. The dots indicate the positions of runs completed by other workers (with no indication of temperature or pressure accuracy). The shaded bands represent divariant melting intervals. The heavy lines are our preferred estimates of the positions of the univariant reactions (a) Or + V = L, and (b) Or + Qz + V = L. The compositions of the liquids involved in these reactions at several pressures are shown by the points a and b in figures 1 and 5.

a starting material, but they gave no information about the runs bracketing this point nor about the impurities in the glass. Shaw (1963) pointed out that there is probably some $Na_2O$ present in glasses prepared by Schairer and Bowen (1955) for the system $K_2O$–$Al_2O_3$–$SiO_2$, although it is apparently less than in gel preparations. Goranson (1938) also used a glass prepared by Schairer for his study of the system Or–$H_2O$ to 3.5 kb. The point S on his curve in figure 4 represents the singular point where sanidine begins to melt congruently in the presence of excess water (but not with water-deficiency, as shown in fig. 1B). Details of the phase relationships around this point have been described by Scarfe, Luth, and Tuttle (1965).

Our best estimates for the positions of the two univariant reaction curves in the system Or–Qz–$H_2O$ are shown by the heavy lines in figure 4, and points on these curves are listed in table 3. The reaction (a), Or + V $\rightleftharpoons$ L, was passed through the point reported by Yoder, Stewart, and Smith (1957) and located at a constant temperature interval of about 10°C above our divariant band Or + L + V. Similarly, the curve for (b), Or + Qz + V $\rightleftharpoons$ L, was drawn about 10°C above our divariant band Or + Qz + L + V and extended downward to just above the divariant band determined by Shaw (1963). With increasing pressure above 6 kb, our preferred curve diverges from that determined by Luth, Jahns, and Tuttle (1964; the lower curve of their shaded interval), the difference amounting to about 20°C at 10 kb. The near-vertical position of their curve is unusual for melting reactions in the granite system as shown by the results in figure 1 of their paper.

TABLE 3

Points on univariant reactions
(a) Or + V = L and (b) Or + Qz + V = L from figure 4

| Pressure Kb | Temperature °C (a) | (b) |
|---|---|---|
| 1 | — | 815 |
| 2 | — | 785 |
| 3 | 925 | 765 |
| 5 | 875 | 740 |
| 10 | 825 | 710 |
| 15 | 795 | 700 |
| 20 | 775 | 697 |

Seki and Kennedy (1965) reported that at pressures above 10 kb, runs with crystalline orthoclase (prepared from $KAlSi_3O_8$ glass) and about 30 volume percent water in sealed capsules yielded muscovite + glass + water, which they interpreted as representing muscovite + fluids or fluids at run conditions. They concluded that the system Or–$H_2O$ is "not remotely binary and the liquids are not in the plane of $KAlSi_3O_8$–$H_2O$." However, in a previous study covering the same pressure-temperature range, Seki and Kennedy (1964) described the coexistence of sanidine + $H_2O$ right up to the reaction curve for the formation of the dense hexagonal phase $KAlSi_3O_8.H_2O$. Why their 1965 runs produced muscovite + fluid remains something of a puzzle, unless they contained such a large excess of water that all orthoclase was hydrolyzed to muscovite during the quench. In our subsolidus runs, sanidine (or sanidine + quartz) persisted for runs of 18 hours or more in the presence of 30 to 40 wt percent water at pressures to 18.5 kb, and only traces of muscovite were produced. We have given reasons for concluding that this muscovite is a quench product, and in the next section we will consider the conditions for the occurrence of muscovite as a primary phase in the join Or–Qz–$H_2O$.

Our results can be interpreted as if Or–$H_2O$ remained a binary system to 18.5 kb. Some departure of liquid and vapor phase compositions from the join Or–$H_2O$ may be expected, as previously discussed, and we would be unable to detect the divariant melting interval so produced since we are already involved with a melting interval because our sanidine composition is $Or_{95}Ab_5$. However, if the vapor phase compositions had departed far from the join Or–Qz–$H_2O$, other subsolidus phases in addition to sanidine and quartz should have been produced, and none were detected, except for the traces of muscovite interpreted as quench products.

## THE SYSTEM $K_2O$-$Al_2O_3$-$SiO_2$-$H_2O$

In order to consider muscovite stability in relation to our results in the system Or–Qz–$H_2O$, we must consider the system $K_2O$-$Al_2O_3$-$SiO_2$-$H_2O$. Phase relationships in the system $K_2O$-$Al_2O_3$-$SiO_2$ at 1 bar were described by Schairer and Bowen (1955), and they are shown in figure 5A. The phases of geological interest are kalsilite (Ks), leucite

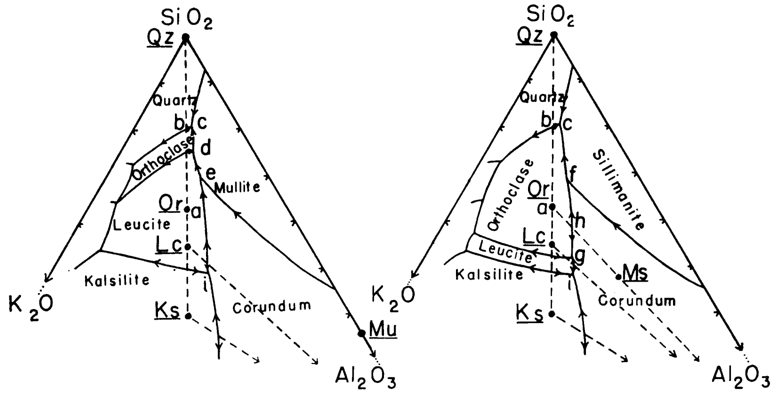

(A) $P_{H_2O}$ = 1 bar (B) $P_{H_2O}$ = 5 kb

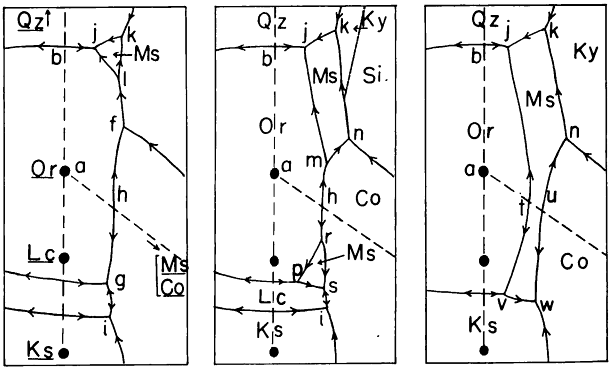

(C) $P_{H_2O}$ = 6 kb (D) $P_{H_2O}$ = 8 kb (E) $P_{H_2O}$ = 11 kb

Fig. 5. Schematic phase diagrams for the system $K_2O$-$Al_2O_3$-$SiO_2$-$H_2O$. A. The dry system after Schairer and Bowen (1955). B. Perspective projection of the vapor-saturated liquidus surface onto the anhydrous base of the quaternary tetrahedron, based mainly on the results of Scarfe, Luth, and Tuttle (1965). The term $P_{H_2O}$ is used for convenience to denote total pressure in the presence of excess $H_2O$; because of the solute content of the vapor phase, $P_{H_2O}$ is actually less than the listed pressure. C, D, and E, are schematic enlargements of a portion of figure 5B, showing the appearance and enlargement of a possible field for primary muscovite with increasing pressure; these diagrams and the indicated pressures are based on figure 6. For abbreviations, see text.

(Lc), orthoclase (Or), polymorphs of silica, corundum (Co), and mullite (Mu). In the presence of water under pressure muscovite (Ms) is an additional phase, and sillimanite (Si, or other polymorphs of $Al_2SiO_5$) replaces mullite on the liquidus as shown in figure 5B. Water dissolves in the silicate liquids, lowering the liquidus temperatures and changing the positions of the vapor-saturated liquidus field boundaries and the shapes of the vapor-saturated liquidus surfaces. Figure 5B is a schematic perspective projection of the vapor-saturated liquidus through the $H_2O$ corner of the quaternary tetrahedron on to the anhydrous system; it is based largely on the results of Scarfe, Luth, and Tuttle (1965) for the system Ks–Qz–$H_2O$, which are indicated in figure 1. Note that in figure 5A, Lc melts congruently while Or melts incongruently, whereas in the presence of excess water at 5 kb, as in figure 5B, Lc melts incongruently and Or melts congruently.

The points a and b in figure 5B represent the projected compositions of the liquid phases involved in the two univariant reactions plotted in figure 4: (a) Or $+$ V $\rightleftharpoons$ L, and (b) Or $+$ Qz $+$ V $\rightleftharpoons$ L, respectively. Similarly, the points c, f, g, and i represent the projected liquid compositions for quaternary univariant reactions involving liquid and vapor. We will be concerned with reaction (c), Or $+$ Qz $+$ Si $+$ V $\rightleftharpoons$ L. The point h is a temperature maximum on the field boundary, giving the projected liquid composition for the ternary univariant reaction (h), Or $+$ Co $+$ V $\rightleftharpoons$ L, in the system Or–Co–$H_2O$; note that muscovite lies in the same ternary system. The dissociation of muscovite is defined by two subsolidus reactions, the ternary (x), Ms $\rightleftharpoons$ Or $+$ Co $+$ V; and the quaternary (y), Ms $+$ Qz $\rightleftharpoons$ Or $+$ Si $+$ V.

*Liquidus phase relationships involving sanidine, quartz, and muscovite.*— Figure 6 is a schematic diagram to illustrate the pattern of phase relationships that brings muscovite to the liquidus as a primary crystalline phase, and figures 5C, D, and E are schematic liquidus diagrams based on figure 6. Four of the liquidus reactions from figure 5B have been plotted as univariant curves in figure 6. The experimentally determined reactions (a) and (b) have been transferred from figures 2 and 3, and the reactions (c) and (h) are in positions estimated from the relative temperatures of the univariant liquids in figures 1 and 5. Experimental determinations of reactions (x) and (y) have suffered from slow reaction rates, and there are a variety of results from which to choose. The curves (x) and (y) in figure 6 are extrapolations of the results of Evans (1965), giving minimum pressures for the stability of muscovite on the liquidus. Velde (1966) determined a point for (x) at 8 kb and about 730°C which lies well above curve (x) in figure 6; the use of Velde's result would give a much higher pressure for $Q_2$ The curves (x) and (y) in figure 6 are located for graphical convenience, as much as anything else, and although the pressure and temperature scales are correct, or approximately correct, for most reactions involving liquid, the muscovite stability field in figure 6 is very schematic. Experimental location of invariant points $Q_1$ and $Q_2$, by working from higher pres-

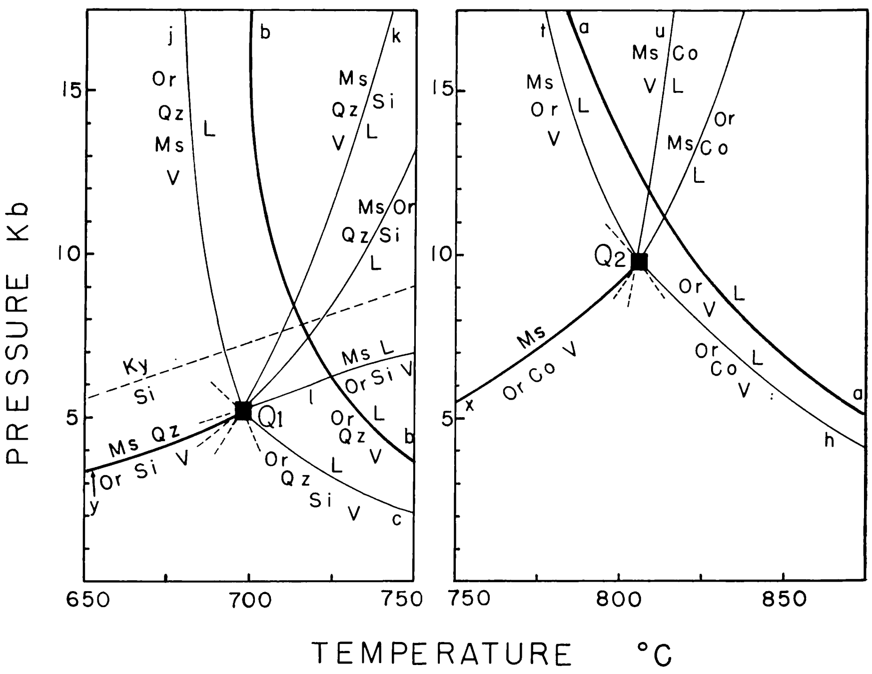

Fig. 6. Schematic pressure-temperature projection for parts of the system $K_2O$–$SiO_2$–$Al_2O_3$–$H_2O$, showing the relationship between the stability of muscovite and melting reactions in the system

A. Conditions for the first appearance of muscovite on the liquidus, in the sub-system Or–Qz–Co–$H_2O$. Reaction (b) taken from figure 4, reaction (y) based on extrapolation of previous studies (see text), kyanite-sillimanite curve from Newton (1966), and the rest schematic. The compositions of the liquids involved in the reactions are shown by the points j, b, k, and l in figure 5.

B. Conditions for the appearance of muscovite on the liquidus in the presence of sanidine and no other crystalline phases, in the sub-system Or–Co–$H_2O$. Reaction (a) taken from figure 4, reaction (x) based on a long extrapolation of previous studies (see text), and the rest schematic. The compositions of liquids involved in the reactions are shown by the points a, h, t, and u in figure 5.

sures where reactions occur more readily in the presence of a liquid phase, offers good prospects for pinning down the high pressure ends of the two subsolidus muscovite reactions, (x) and (y).

The liquidus surface shown in figure 5B moves to lower temperatures with increasing pressure in the presence of excess $H_2O$, and the muscovite dissociation curves (x) and (y) rise to higher temperatures until they intersect the liquidus reactions, as shown in figure 6. The first intersection, between dissociation curve (y) and reaction (c), generates the quaternary invariant point $Q_1$, as shown in figure 6A. At higher pressures, the isobaric invariant liquid c of figure 5B is replaced by a small field for primary muscovite, as shown in figure 5C. The three liquids, j, k, and l, which replace the single liquid, c, are represented in figure 6A by three univariant curves extending to higher pressures above the invariant point. The arrangement of the univariant curves was determined following the methods of Schreinemakers (1916) and Zen (1966), but their actual positions need experimental determination. The fifth curve, with vapor absent, represents a liquid beneath the vapor-saturated liquidus surface. Figure 6A may be compared with figure 2 of Segnit and Kennedy (1961) who determined melting curves for mixtures with muscovite-quartz-water compositions, with figure 10 of Evans (1965), and with figure 3 of Seki and Kennedy (1965).

It is assumed that the temperature of liquid g in figures 5B and 5C is somewhat higher than that of liquid f. With increasing pressure, the liquids l and k of figure 5C rise to higher temperatures, as indicated in figure 6A, and the next change occurs when liquid l reaches liquid f (fig. 5C; not shown in fig. 6), generating another invariant point involving the muscovite dissociation reaction (x). This invariant point is not shown in figure 6. At higher pressures, liquids l and f are replaced by m and n, as shown in figure 5D. There follows another invariant point where dissociation reaction (x) intersects univariant reaction (g), which is not plotted in figure 6. This causes liquid g to be replaced by liquids s, p, and r, surrounding a second field for primary muscovite, as shown in figure 5D. These two invariant points are quaternary, but degenerate, because Ms composition lies in the plane Or–Co–$H_2O$.

The univariant reactions involving liquids m and r in figure 5D are identical in pressure-temperature projection with the ternary muscovite dissociation reaction (x) in figure 6B. Therefore, with increasing pressure, the liquids m and r of figure 5D move together, becoming coincident with the point h at the pressure where intersection occurs between reactions (x) and (h) in figure 6B. This produces a ternary invariant point $Q_2$, with three additional univariant curves; two of these appear as temperature maxima, t and u, in figure 5E. At pressures greater than $Q_2$, muscovite has a continuous liquidus field as indicated in figure 5E. This extends beneath the vapor-saturated liquidus surface of figure 5B as indicated by the vapor-absent curves in figure 6. The transition from sillimanite to kyanite (Ky) is shown in figures 5D and 5E, and the transition curve is plotted in figure 6A (Newton, 1966); in figure 6A, the abbreviation Si is used for both sillimanite and kyanite in order to prevent crowding of the diagram.

The exchange of liquids p, s, and i in figure 5D for the liquids v and w in figure 5E involves other invariant points related to the breakdown of leucite by the reaction Lc $\rightleftharpoons$ Ks + Or (Scarfe, Luth, and Tuttle, 1965). We have worked out a schematic pressure-temperature projection for the whole system Ks–Qz–Co–$H_2O$, which links together figures 6A and 6B and incorporates the additional invariant points discussed in the preceding analysis; any interested reader may do the same using our figures as a basis. We decided to present only the two invariant points required for our discussion, as in figure 6, because each additional point complicates the diagrams with another family of univariant lines.

Figures 5 and 6, although based on a minimum of experimental data, provide some limits for the appearance of primary muscovite on the composition joins Or–$H_2O$ and Or–Qz–$H_2O$ of the quaternary system $K_2O$–$Al_2O_3$–$SiO_2$–$H_2O$. Muscovite can not occur on the liquidus on these joins at pressures lower than the invariant points $Q_2$ and $Q_1$, respectively. Thus, muscovite can crystallize along with sanidine and quartz only at pressures greater than about 5 or 6 kb, and muscovite can crystallize along with sanidine in the absence of other crystalline phases only above 10 or 11 kb. For muscovite to appear as a primary phase on the liquidus of the composition join Or–Qz–$H_2O$, even higher pressures are required, because the liquids j and t of figure 5E must cross the composition join. According to figures 6A and 6B, the reactions (j) and (t) remain below (b) and (a), respectively, at least to pressures of 15 kb. However, the temperatures of reactions (h), (c), (j), and (t) are not known, and if these were, in fact, located closer to the reactions (b) and (a), then there is a prospect that (j) and (b) in figure 6A, and (t) and (a) in figure 6B, could merge at singular points, which would correspond in figure 5E to the points where j and t meet b and a, respectively, and cross over the join Or–Qz–$H_2O$. The curves (j) and (t) need experimental determination in order to establish whether or not the muscovite field does cross the join Or–Qz–$H_2O$.

## DISCUSSION

We do not intend to review the applications of the phase relationships in this system to petrological problems, because these have been discussed in most of the previous papers presenting experimental results, but one feature of figures 5 and 6 merits comment. The plane joining the line Ks–Qz to the vapor phase remains a thermal barrier to the highest pressures shown. In figure 5, the temperature maxima on the field boundaries remain on the line Ks–Qz only if the vapor phase composition remains in the join Ks–Qz–$H_2O$, and this assumption is implicit in the diagrams and the preceding analysis of the phase relationships. If the assumption is accepted, then we conclude that in the system $K_2O$–$Al_2O_3$–$SiO_2$–$H_2O$, the only liquids that can precipitate muscovite during fractional crystallization are those on the $Al_2O_3$ side of the join Ks–Qz, that is, corundum-normative liquids. However, as mentioned previously, the vapor phase may contain up to 10 wt percent solute at 10 kb pressure, and this could probably reach about 15 percent at 15 kb. If the vapor phase were enriched in $K_2O$–$SiO_2$ compared to the join Ks–Qz, then the thermal barrier on the vapor-saturated liquidus surface would also be shifted toward $K_2O$–$SiO_2$, and liquids with compositions on the join Ks–Qz–$H_2O$ would precipitate muscovite during crystallization, if the pressure were above that of the appropriate invariant points. This is a possible explanation for the traces of quench muscovite in some of our runs, although it does not explain the subsolidus muscovite, nor does it explain the muscovite present in runs quenched from temperatures above 800°C at pressures of 5 and 7.5 kb (table 1), runs well above the stability limit of muscovite (see fig. 6B). Precipitation of muscovite from vapor during the quench thus remains our preferred interpretation.

## ACKNOWLEDGMENTS

We gratefully acknowledge the following support: National Science Foundation for Grant GA-923; Advanced Research Project Agency for the assistantship for J. K. Robertson and for some of the apparatus used. We thank R. C. Newton for critical review of the manuscript.

## REFERENCES

Boettcher, A. L., and Wyllie, P. J., 1967, Hydrothermal melting curves in silicate-water systems at pressures greater than 10 kbars: Nature, v. 216, p. 572-573.

——— 1968a, Melting of granite with excess water to 30 kbars pressure: Jour. Geology, v. 76, p. 235-244.

——— 1968b, The calcite-aragonite transition measured in the system $CaO$–$CO_2$–$H_2O$: Jour. Geology, v. 76, p. 314-330.

——— 1969a, Phase relationships in the system $NaAlSi_3O_8$–$SiO_2$–$H_2O$ to 35 kilobars pressure. Am. Jour. Sci., v. 267, in press.

——— 1969b, The system $CaO$–$SiO_2$–$CO_2$–$H_2O$: III.—Second critical end-point on the melting curve: Geochim. et Cosmochim. Acta, v. 33, in press.

Boyd, F. R., and England, J. L., 1960, Apparatus for phase equilibrium measurements at pressures up to 50 kbars and temperatures up to 1750°C: Jour. Geophys. Research, v. 65, p. 741-748.

Burnham, C. W., 1967, Hydrothermal fluids at the magmatic stage, *in* Barnes, H. L., ed., Geochemistry of hydrothermal ore deposits: New York, Holt, Rinehart, and Winston, Inc., p. 34-75.

Evans, B. W., 1965, Application of a reaction rate method to the breakdown equilibria of muscovite and muscovite plus quartz: Am. Jour. Sci., v. 263, p. 647-667.

Goranson, R. W., 1938, Silicate water systems. Phase equilibria in the $NaAlSi_3O_8$–$H_2O$ and $KAlSi_3O_8$–$H_2O$ systems at high temperatures and pressures: Am. Jour. Sci., 5th ser., v. 35, p. 71-91.

Green, T. H., and Ringwood, A. E., 1968, Genesis of the calc-alkaline igneous rock suite: Contr. Mineralogy Petrology, v. 18, p. 105-162.

Kennedy, G. C., Wasserburg, G. J., Heard, H. C., and Newton, R. C., 1962, The upper three phase region in the system $SiO_2$–$H_2O$: Am. Jour. Sci., v. 260, p. 501-521.

Lindsley, D. H., 1966, Melting relations of $KAlSi_3O_8$: effect of pressure up to 40 kbars: Am. Mineralogist, v. 51, p. 1793-1799.

——— P-T projection for part of the system kalsilite-silica: Carnegie Inst. Washington Year Book 65, p. 244-247.

Luth, W. C., 1968, The influence of pressure on the composition of eutectic liquids in the binary systems sanidine-silica and albite-silica: Carnegie Inst. Washington Year Book 66, p. 480-484.

Luth, W. C., and Ingamells, O., 1965, Gel preparation of starting materials for hydrothermal experimentation: Am. Mineralogist, v. 50, p. 255-258.

Luth, W. C., Jahns, R. H., and Tuttle, O. F., 1964, The granite system at pressures of 4 to 10 kbars: Jour. Geophys. Research, v. 69, p. 759-773.

Newton, R. C., 1966, Kyanite-sillimanite equilibrium at 750°: Science, v. 151, p. 1222-1225.

Orville, P. M., 1963, Alkali ion exchange between vapor and feldspar phases: Am. Jour. Sci., v. 261, p. 201-237.

Piwinskii, A. J., 1968, Experimental studies of igneous rock series; central Sierra Nevada batholith, California: Jour. Geology, v. 76, p. 548-570.

Scarfe, C. M., Luth, W. C., and Tuttle, O. F., 1965, An experimental study bearing on the absence of leucite in plutonic rocks: Am. Mineralogist, v. 51, p. 726-735.

Schairer, F. J., and Bowen, N. L., 1955, The system $K_2O$–$Al_2O_3$–$SiO_2$: Am. Jour. Sci., v. 253, p. 681-746.

Schreinemakers, F. A. H., 1916, In- mono- and divariant equilibria: Amsterdam Acad. Sci., Proc., v. 18, p. 820-828.

Segnit, R. E., and Kennedy, G. C., 1961, Reactions and melting relations in the system muscovite-quartz at high pressures: Am. Jour. Sci., v. 259, p. 280-287.

Seki, Y., and Kennedy, G. C., 1964, The breakdown of potassium feldspar, $KAlSi_3O_8$, at high temperatures and high pressures: Am. Mineralogist, v. 49, p. 1688-1706.

———— 1965, Muscovite and its melting relations in the system $KAlSi_3O_8$–$H_2O$: Geochim. et Cosmochim. Acta., v. 29, p. 1077-1083.

Shaw, H. R., 1963, The four-phase curve sanidine-quartz-liquid-gas between 500 and 4000 bars: Am. Mineralogist, v. 48, p. 883-896.

Spengler, C. J., ms., 1965, The upper three phase region in a portion of the system $KAlSi_2O_6$–$SiO_2$–$H_2O$ at water pressures from 2 to 7 kbars: Ph.D. thesis, Penn. State Univ., University Park, Pa.

Stewart, D. B., 1967, Four phase curve in the system $CaAl_2Si_2O_8$–$SiO_2$–$H_2O$ between 1 and 10 kbars: Schweizer min. pet. Mitt., v. 47, p. 35-59.

Tuttle, O. F., and Bowen, N. L., 1958, Origin of granite in light of experimental studies: Geol. Soc. America Mem. 74, 153 p.

Velde, B., 1966, Upper stability of muscovite: Am. Mineralogist, v. 51, p. 924-929.

Wyllie, P. J., and Boettcher, A. L., 1969, Liquidus phase relationships in the system $CaO$–$CO_2$–$H_2O$ to 40 kbars pressure with petrological applications: Am. Jour. Sci., v. 267-A, Schairer v., p. 489-508.

Yoder, H. S., Stewart, D. B., and Smith, J. R., 1957, Ternary feldspars: Carnegie Inst. Washington Year Book 56, p. 206-214.

Zen, E-an, 1966, Construction of pressure-temperature diagrams for multicomponent systems after the method of Schreinemakers—a geometric approach: U.S. Geol. Survey Bulletin 1225, 56 p.